

***Ab Initio* Design of High-*k* Dielectrics:  $\text{La}_x\text{Y}_{1-x}\text{AlO}_3$** Stephen A. Shevlin,<sup>\*</sup> Alessandro Curioni, and Wanda Andreoni<sup>†</sup>*IBM Research, Zurich Research Laboratory, 8803 Rüschlikon, Switzerland*

(Received 16 July 2004; published 13 April 2005)

We use calculations based on density-functional theory in the virtual crystal approximation for the design of high-*k* dielectrics, which could offer an alternative to silicon dioxide in complementary metal-oxide semiconductor devices. We show that aluminates  $\text{La}_x\text{Y}_{1-x}\text{AlO}_3$  alloys derived by mixing aluminum oxide with lanthanum and yttrium oxides have unique physical attributes for a possible application as gate dielectrics when stabilized in the rhombohedral perovskite structure, and which are lost in the orthorhombic modification. Stability arguments locate this interesting composition range as  $0.2 < x < 0.4$ . Phase separation in microdomains is shown to have the tendency to further enhance the dielectric constant. We propose this as a novel family of high-*k* dielectrics deserving experimental exploration.

DOI: 10.1103/PhysRevLett.94.146401

PACS numbers: 71.15.Pd, 77.22.-d

One of the most critical and challenging problems silicon technology is currently facing is that of extending the scaling down of complementary metal-oxide semiconductor field-effect transistors (FETs) to a physical thickness of 1–2 nm [1]. Given that silicon dioxide, the gate dielectric commonly used, suffers dielectric breakdown in this size regime, an alternative material will have to replace it [2,3]. Clearly this material should have a dielectric constant  $\epsilon_0$  higher than that of silicon dioxide, and specifically  $\epsilon_0 \sim 25$  is required for the next generation. This is the criterion that has guided the experimental search for alternative oxides and that has led to the proposal of binary compounds [4], e.g., alumina, zirconia, and hafnia, and of a few ternary compounds [3,5,6] as possible candidates. This search is far from complete, and intense experimental investigation is also being pursued on the basis of other concomitant requirements for device performance, e.g., high electron mobility in the channel, high thermal stability, and a conduction band offset larger than  $\sim 1$  eV.

On the theoretical side, linear response theory [7] based on density-functional theory (DFT) [8] is the general approach that has been adopted to calculate and analyze the static dielectric constant of several of the above materials [9,10]. It is the aim of this Letter to go one step further and show how DFT calculations can indeed be used not only as a probe of the microscopic mechanisms responsible for the variation of the dielectric constant with composition and structure but also as a tool for the design of novel dielectric materials. Our investigation focuses on compounds derived from aluminum oxide by alloying it with either lanthanum or yttrium oxide. Indeed, while neither lanthanum nor yttrium oxide are believed to be viable candidates for an alternative to silicon dioxide, lanthanum aluminates are currently under serious consideration [6]. Our study of the interplay between structural and dielectric properties of the aluminates reveals the intriguing dependence of the latter on specific phonon modes and leads us to propose a series of quaternary compounds  $\text{La}_x\text{Y}_{1-x}\text{AlO}_3$  of a well-defined concentration range as novel high-*k* dielectrics with especially interesting attributes. They possess dielec-

tric constants with average values close to the requirements of the next-generation FETs, and that can be enhanced by exploiting their characteristic anisotropy and tuned to minimize the detrimental effect of phonon scattering on the electron mobility in the channel [11]. Moreover, they are wide-gap insulators with band gaps larger than the parent ternary compounds.

We present calculations on aluminum oxide ( $\text{Al}_2\text{O}_3$ ), lanthanum aluminate ( $\text{LaAlO}_3$ ), yttrium aluminate ( $\text{YAlO}_3$ ), and quaternary solid-solution alloys,  $\text{La}_x\text{Y}_{1-x}\text{AlO}_3$ . Our DFT computational scheme is based on local-density exchange and correlation functionals [12] and utilizes the pseudopotential (PS) method to reduce the electronic problem to that of valence electrons whose wave functions are expanded in plane waves up to an energy cutoff of 120 Ry. Norm-conserving angular-momentum-dependent PSs are derived with the Martins-Troullier method [13]; in particular, to guarantee transferability, Y and La are treated as systems with 11 valence electrons (semicore PS). The local-density approximation (LDA) functionals were preferred over gradient-corrected ones because of their better performance in the representation of the structural, vibrational, and dielectric properties of both  $\text{Al}_2\text{O}_3$  and  $\text{LaAlO}_3$ . However, calculations based on the Perdew-Burke-Ernzerhof approximation [14] were used to verify the LDA prediction of structural energy differences. For the modeling of an alloy of generic composition, we have adopted the virtual crystal approximation (VCA), which implies preserving the same crystalline unit cells as the ternary compounds and replacing the heavy metal cation with a suitable virtual atom. In spite of the long-standing extensive use of the VCA concept within the PS framework [15], only lately has it become a reliable approach due to recent formulations [16,17], which are consistent with the “modern” PS schemes. Our implementation follows the idea introduced in [16], which is consistent with our DFT norm-conserving PS method (DFT-VCA). For each compound, we optimize both lattice parameters and internal coordinates. Within the linear response DFT approach [7,18], we obtain the vibrational

TABLE I. Calculated lattice parameters (theory) of  $\text{LaAlO}_3$  and  $\text{YAlO}_3$  in the LAP and YAP structures and experimental data (Ref. [19] for  $\text{LaAlO}_3$  and Ref. [20] for  $\text{YAlO}_3$ ).

LAP	$a(\text{\AA})$		$\alpha$			
	Theory	Exp	Theory	Exp	Theory	Exp
$\text{LaAlO}_3$	5.29	5.35	60.1	60.1		
$\text{YAlO}_3$	5.10	...	61	...		
YAP	$a(\text{\AA})$		$b/a$		$c/a$	
	Theory	Exp	Theory	Exp	Theory	Exp
$\text{YAlO}_3$	5.10	5.18	1.03	1.03	1.42	1.42

properties and determine the dielectric constant. The performance of our VCA PS scheme was tested against calculations of ordered alloys.

The room-temperature structure of  $\text{LaAlO}_3$  is the rhombohedral perovskite (PV) [19] (“LAP”). Our computational scheme performs well in determining its structural characteristics (Table I). As the  $\alpha$  modification of  $\text{Al}_2\text{O}_3$  [21] is also rhombohedral, this facilitates comparison of the physical properties of the two compounds and the analysis of the effects of alloying. The static dielectric constant  $\epsilon_0$  of  $\alpha\text{-Al}_2\text{O}_3$  (see Table II) is dominated by the contribution of the ionic polarizability ( $\sim 70\%$ ), in agreement with experimental data [22]. Also, the anisotropy index  $\eta = (\epsilon_{0,\parallel}/\epsilon_0 - 1)$ , where  $\epsilon_{0,\parallel}$  is the component along the rhombohedral axis, is significant:  $\eta = 0.140$  [22] from experiment and 0.134 in our calculations. In addition, a specific low-frequency phonon ( $394\text{ cm}^{-1}$ ) dominates the component  $\epsilon_{0,\parallel}$  and is the one responsible for its anisotropy. This vibration involves the out-of-phase collective oscillations of the aluminum ions and the associated oxygen atoms, along the rhombohedral axis.

On passing from  $\text{Al}_2\text{O}_3$  to  $\text{LaAlO}_3$ , we find that  $\epsilon_0$  increases by a factor of  $\sim 2.5$ , in agreement with experiment (see Table II). Again its value turns out to be dominated by the contribution of the ionic polarizability ( $\sim 80\%$  of its average value), and its component along the rhombohedral axis is essentially due to one specific phonon ( $A_{2u}$ ), at a much lower frequency ( $\sim 180\text{ cm}^{-1}$ ) than in the binary alloy. Our predicted frequency (the lowest of the IR spectrum) is in excellent agreement with the values observed experimentally ( $183$  [26] and  $185\text{ cm}^{-1}$  [27]). Interestingly, this vibration is of the same nature as the one at  $394\text{ cm}^{-1}$  in the binary alloy, but only the heavy metal ions move out of phase with the oxygens, whereas the lighter aluminum ions move in phase. This suggests that the major mechanism by which the partial substitution of Al with La atoms drives an increase of the dielectric constant is the softening of a specific IR-active phonon. On the other hand, the anisotropy of  $\epsilon_0$  becomes weak ( $\eta = 0.015$ ), consistent with the highly isotropic nature of the (pseudocubic) crystal structure (Table I).

The above observations have guided us in the search for compounds with higher  $\epsilon_0$ . The most natural operation

TABLE II. Average  $\epsilon_0$  calculated for  $\alpha\text{-Al}_2\text{O}_3$ ,  $\text{LaAlO}_3$ , and  $\text{YAlO}_3$ . Experimental data for the aluminates refer to both single crystals and amorphous materials.

$\text{Al}_2\text{O}_3$	Theory	Exp [22]			
		LAP	LAP	YAP	YAP
	10.4				
$\text{LaAlO}_3$	Theory	Exp [23]; [24]	Theory	Exp [25]	
	25.8	24.5; 21–24	...	...	
$\text{YAlO}_3$	Theory	Exp [23]; [24]	Theory	Exp [25]	
	31.7	...	15.7	16	

appeared to be the substitution of the heavy metal in the LAP with one that would soften further—but not towards structural instability—the critical  $A_{2u}$  IR phonon, and ensure an increase in anisotropy. Although counterintuitive, replacing La in the aluminate with a lighter atom such as Y provides these desired characteristics. Table II reveals a substantial increase of  $\epsilon_0$ , which is exclusively due to a further softening of the  $A_{2u}$  phonon (now at  $\sim 110\text{ cm}^{-1}$ ), whose intensity, on the other hand, is not affected by the heavy metal substitution. This is shown in Fig. 1. In contrast, the remainder of the spectrum is shifted slightly to higher frequencies, consistent with Y being lighter than La. The nature of the  $A_{2u}$  mode is intriguing: the heavy metal atom vibrates out of phase relative to the anions in its 12-fold coordination shell so that the smaller the size of the engaged ion, the lower the frequency. Moreover, the greater distortion of the rhombohedral structure from the cubic one in the Y compound leads to a much larger splitting between the  $A_{2u}$  and the  $E_u$  modes ( $\sim 100$  vs  $\sim 10\text{ cm}^{-1}$ ). As a consequence,  $\epsilon_0$  possesses an anisotropy, which is dramatically larger than in the La analog ( $\eta = 0.86$ ).

Unfortunately,  $\text{YAlO}_3$  is not stable at room temperature as a rhombohedral PV, but rather assumes the orthorhombic structure [20] (YAP) in which the dielectric constant is dramatically lower [25] (see Table II). Our calculations result in a value of the dielectric constant that compares very well with experiment and reveal that its decrease of the dielectric constant is predominantly determined by the hardening of the IR-active phonons. This behavior can be ascribed to the different alignment (and relative orienta-

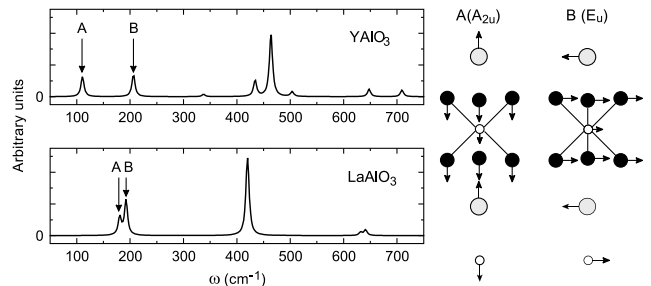


FIG. 1. Calculated infrared spectrum for  $\text{LaAlO}_3$  and  $\text{YAlO}_3$  in the LAP structure. On the right-hand side, the atomic displacements in the unit cell are depicted, which correspond to the  $A(A_{2u})$  and  $B(E_u)$  phonons.

tion) of the structural units in the two PVs. The scenario exhibited by these materials is distinct from that identified in Ref. [10] for Zr silicates, in which different structural units are present with different cationic coordination so that their relative concentration can be tailored to enhance the dielectric response.

From the above results, the idea emerges of trying to stabilize the rhombohedral modification of  $\text{YAlO}_3$  by doping it with La, thus giving rise to a new family of quaternary compounds. As explained above, our calculations for these alloys are based on the DFT-VCA, a valid approach to disordered solid solutions that allows one to quantitatively determine compositional phase boundaries and structural preferences [16,17]. Physically, our model virtual alloys represent a well-defined limit, that of full (uniform) positional disorder on the lattice sites of the heavy metal cation, where La or Y are supposed to reside with relative probability proportional to their relative concentration. In this limit, we approximately locate the range of stability of the LAP structure and determine how the dielectric constant changes with composition.

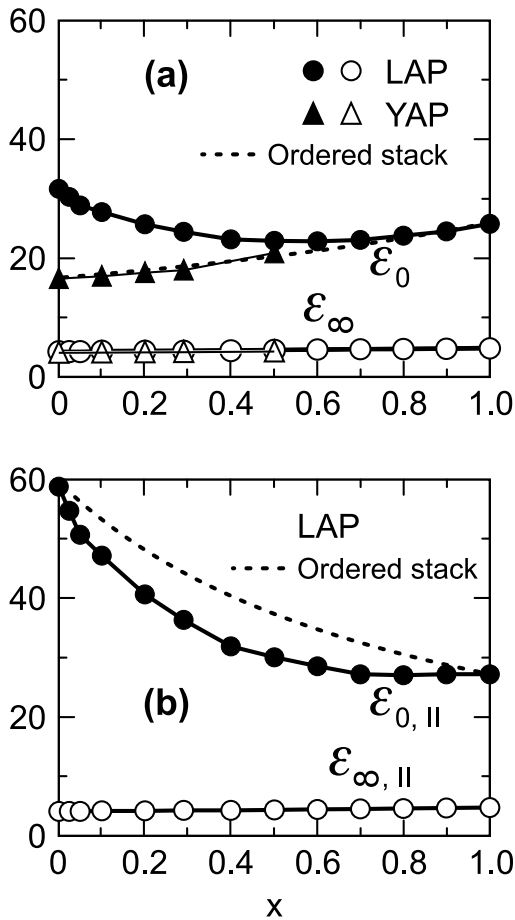


FIG. 2.  $\text{La}_x\text{Y}_{1-x}\text{AlO}_3$ : Calculated dielectric constants, both static and high-frequency values, vs lanthanum concentration. (a) Average values; (b) maximum components.

Structural energy differences, including the zero-point energy contributions, indicate that the YAP structure is more stable up to  $x \sim 0.2$ , that it may coexist with the LAP up to about midcomposition, and then the LAP phase should become the only stable one. Our findings for the behavior of the dielectric constant as a function of composition (Fig. 2) [28] reveal a whole range in which mixing could be very effective in enhancing the screening. Three main characteristics emerge from Fig. 2: (i) the insensitivity of the high-frequency value to composition (e.g., in the LAP from  $\sim 4.4$  in  $\text{YAlO}_3$  to  $\sim 4.8$  in  $\text{LaAlO}_3$ ) as well as on the structure (for  $\text{YAlO}_3$  from  $\sim 4.1$  in the YAP to  $\sim 4.4$  in the LAP); (ii) the predominant weight of the ionic contribution, and as a consequence (iii) the critical dependence of  $\epsilon_0$  on the structure in the Y-rich region, where the two phases are clearly distinct. In the rhombohedral phase [Fig. 2(a)]  $\epsilon_0$  shows an anomalous dependence on the La content with a minimum near midcomposition: This is due to the contrasting behavior of the  $A_{2u}$  mode, which hardens for increasing La content, and that of the remainder of the IR spectrum, which is more sensitive to the mass increase of the metal ion. Moreover, as expected, (iv) the degree of anisotropy in the LAP decreases from the Y-rich to the La-rich compounds.

Going beyond the VCA so as to better describe the “real” alloys and understand the subtle effects of ordering is important [29]. Given that, however, an exhaustive investigation is for the moment prohibitive from first principles, we adopt here another view and consider the opposite limit to our virtual alloys that is represented by an ordered stack of  $\text{LaAlO}_3$  and  $\text{YAlO}_3$  layers with thickness proportional to  $x$  and  $(1-x)$ , respectively. Physically, this corresponds to having a stack of capacitors in series; the dielectric constant can be easily calculated once interface effects are neglected. We consider two cases:  $\text{YAlO}_3$  in either the YAP or the LAP structure. In the former, the calculated dielectric constant closely corresponds to the VCA values, thus revealing an insignificant role of positional disorder [Fig. 2(a)]. In the latter [Fig. 2(b)], on the contrary, a non-negligible deviation is observed, and the effect of positional disorder appears to correspond to a decrease of the dielectric constant. Therefore, one can reasonably expect that in the real system, where different microdomains may coexist, the desired enhancement in the region of stability of the rhombohedral phase is higher than what the DFT-VCA predicts. On the other hand, the difference of screening in an amorphous or a crystalline such material is minimal, as shown by the measured dielectric constant of  $\text{LaAlO}_3$  samples (Table II).

In conclusion, after gaining an unprecedented understanding of the dielectric properties of the La and Y aluminates, we have identified the factors that are crucial for the characteristics of the dielectric screening and hence for the design of novel materials with the same elemental components. On these grounds, we propose a series of

novel quaternary compounds ( $\text{La}_x\text{Y}_{1-x}\text{AlO}_3$ , in the range  $0.2 < x < 0.4$ ) that are expected to exhibit very interesting properties: (i) The average values of the static dielectric constants are close to the one required for next-generation FETs; (ii) The anisotropy of the dielectric constants is strong and mainly due to low-frequency phonons along the rhombohedral axis that are sufficiently split from their in-plane counterparts. This feature, which is expected to be present in crystalline samples, could be realized in thin films by growing these alloys epitaxially, and exploited to help achieve high screening in the region perpendicular to the channel without forcedly amplifying the effect of phonon scattering on the electron mobility in the channel. Moreover, (iii) for the proposed range of compositions our calculations indicate an increase in the band gap of  $\sim 1$  eV with respect to  $\text{LaAlO}_3$ , and thus an increase of the conduction band offset with silicon ( $\sim 1$ – $2$  eV in  $\text{LaAlO}_3$  [30]) is expected, which is beneficial for the electrical behavior; and (iv) regarding the properties of the oxide interface with silicon, one could argue—on the basis of the known behavior of yttria [31]—that those of Y-rich YLa aluminates should not be worse than those of La aluminates themselves, on which great improvements have recently been achieved [6].

Our approach shows that a new avenue is opening up in the search of a suitable high- $k$  dielectric as replacement of silicon dioxide and which, at least during the early phases, relies on virtual material design using DFT computer simulations. We believe that the results presented here are very interesting and should foster experimental verification of our predictions as well as further work in other multinary aluminates in the rhombohedral perovskite structure. Beyond the specific application as gate oxides of FETs herein discussed, these novel dielectrics could be of special interest for other technologies, e.g., as substrates of high-temperature superconductors or as microwave dielectric resonators.

---

\*Now at Joint Institute for Computational Science, Computer Science and Mathematics Division, Oak Ridge National Laboratory, Oak Ridge, TN 37831-6008, USA.

†Corresponding author.

Electronic address: and@zurich.ibm.com

- [1] P. S. Peercey, *Nature* (London) **406**, 1023 (2000).  
 [2] A. I. Kingon, J.-P. Maria, and S. K. Streiffer, *Nature* (London) **406**, 1032 (2000).  
 [3] G. D. Wilk, R. M. Wallace, and J. M. Anthony, *J. Appl. Phys.* **89**, 5243 (2001).  
 [4] See, e.g., E. P. Gusev *et al.*, *Microelectron. Eng.* **59**, 341 (2001); M. Copel *et al.*, *Appl. Phys. Lett.* **78**, 2670 (2001); S. Zafar *et al.*, *ibid.* **81**, 2608 (2002); S. Ramanathan *et al.*, *ibid.* **79**, 2621 (2001); A. Javey *et al.*, *Nat. Mater.* **1**, 241 (2002); H. Kim, P. C. McIntyre, and K. C. Saraswat, *Appl. Phys. Lett.* **82**, 106 (2003).  
 [5] See, e.g., H. Watanabe, *Appl. Phys. Lett.* **81**, 4221 (2002); H. Takeuchi and T.-J. King, *ibid.* **83**, 788 (2003); P. Panchaipetch *et al.*, *J. Vac. Sci. Technol.* **22**, 395 (2004).  
 [6] W. Xiang *et al.*, *J. Appl. Phys.* **93**, 533 (2003); Xu-bing Lu *et al.*, *ibid.* **94**, 1229 (2003).  
 [7] P. Giannozzi *et al.*, *Phys. Rev. B* **43**, 7231 (1991).  
 [8] R. G. Parr and W. Yang, *Density Functional Theory of Atoms and Molecules* (Oxford University Press, New York, 1989).  
 [9] X. Zhao and D. Vanderbilt, *Phys. Rev. B* **65**, 233106 (2002).  
 [10] G.-M. Rignanese *et al.*, *Phys. Rev. Lett.* **89**, 117601 (2002).  
 [11] M. V. Fischetti and S. E. Laux, *Appl. Phys. Lett.* **76**, 2277 (2000); M. V. Fischetti, D. A. Neumayer, and E. A. Cartier, *J. Appl. Phys.* **90**, 4587 (2001).  
 [12] D. M. Ceperley and B. I. Alder, *Phys. Rev. Lett.* **45**, 566 (1980); J. P. Perdew and A. Zunger, *Phys. Rev. B* **23**, 5048 (1981).  
 [13] N. Troullier and J. L. Martins, *Phys. Rev. B* **43**, 1993 (1991); L. Kleinman and D. M. Bylander, *Phys. Rev. Lett.* **48**, 1425 (1982).  
 [14] J. P. Perdew, K. Burke, and M. Ernzerhof, *Phys. Rev. Lett.* **77**, 3865 (1996).  
 [15] *Solid State Physics*, edited by H. Ehrenreich, F. Seitz, and D. Turnbull (Academic Press, New York, 1970), Vol. 24.  
 [16] N. J. Ramer and A. M. Rappe, *Phys. Rev. B* **62**, R743 (2000); *Fundamental Physics of Ferroelectrics*, edited by R. E. Cohen, AIP Conf. Proc. No. 535 (AIP, Melville, 2000), pp. 95–101.  
 [17] L. Bellaïche and D. Vanderbilt, *Phys. Rev. B* **61**, 7877 (2000).  
 [18] Most calculations were made using the PWSCF code (S. Baroni *et al.*, SISSA, Trieste, Italy), <http://www.pwscf.org>.  
 [19] S. Geller and V. B. Bala, *Acta Crystallogr.* **9**, 1019 (1956); S. Bueble *et al.*, *Surf. Sci.* **400**, 345 (1998).  
 [20] S. Geller and E. A. Wood, *Acta Crystallogr.* **9**, 563 (1956).  
 [21] R. N. G. Wyckoff, *Crystal Structures* (Interscience, New York, 1964), Vol. II.  
 [22] A. S. Barker, *Phys. Rev.* **132**, 1474 (1963).  
 [23] G. A. Samara, *J. Appl. Phys.* **68**, 4214 (1990).  
 [24] B.-E. Park and H. Ishiwara, *Appl. Phys. Lett.* **79**, 806 (2001).  
 [25] S.-Y. Cho, I.-T. Kim, and K. S. Hong, *J. Mater. Res.* **14**, 114 (1999).  
 [26] P. Calvani *et al.*, *Physica* (Amsterdam) **181C**, 289 (1991).  
 [27] Z. M. Zhang *et al.*, *J. Opt. Soc. Am. B* **11**, 2252 (1994).  
 [28] Convergence was achieved in both structures in terms of the reciprocal space mesh and calculations of  $\text{LaAlO}_3$  (which is unstable in the orthorhombic modification) in the YAP unit cell reproduced those in the LAP unit cell.  
 [29] See, e.g., N. Marzari, S. de Gironcoli, and S. Baroni, *Phys. Rev. Lett.* **72**, 4001 (1994); L. Bellaïche, A. Garcia, and D. Vanderbilt, *ibid.* **84**, 5427 (2000); H. Grinberg, V. R. Cooper, and A. M. Rappe, *Nature* (London) **419**, 909 (2002).  
 [30] P. W. Peacock and J. Robertson, *J. Appl. Phys.* **92**, 4712 (2002); L. F. Edge *et al.*, *Appl. Phys. Lett.* **84**, 726 (2004).  
 [31] B. W. Busch *et al.*, *Appl. Phys. Lett.* **79**, 2447 (2001); M. Copel *et al.*, *ibid.* **81**, 4227 (2002).